Acta
Technica
Jaurinensis

Vol. 12, No. 2, pp. 161-177, 2019
DOI: 10.14513/actatechjaur.v12.n2.501
Available online at acta.sze.hu

Comparative Analysis of Axlebox Accelerations in Correlation with Track Geometry Irregularities

Cs. Ágh[1]

[1]Széchenyi István University, Department of Transport Infrastructure and Water Resources Engineering
Egyetem tér 1, 9026 Győr, Hungary
e-mail: agh.csaba@sze.hu

Abstract: Stochastic track irregularities influence additional dynamic forces developed in the vehicle-track interaction that lead to faster deterioration of track. For economical track maintenance it is important to understand the relationship between the irregularities recorded by conventional track geometry measuring car and the resulting dynamic vehicle responses. This paper focuses on the correlation between lateral and vertical axlebox accelerations and differently processed track geometry parameters based on a real measurement run on straight track. Decolouring of chord-offset measurement results was performed and derivatives of track geometry parameters were calculated for comparison. Those track geometry parameters have been selected which provide the most accurate information about the recorded wheelset accelerations caused by track geometry irregularities, eg. second order derivative of cross level.

Keywords: track geometry; axlebox acceleration; vehicle response; decolouring

1. Introduction

The deterioration of the railway track is primarily caused by static and dynamic forces transferred from the vehicles. The railway track alignment always deviates from nominal geometry; it contains vertical and lateral geometric irregularities. The railway wheelset passing through the geometric defects is forced to ‘follow’ these irregularities, because of that the railway vehicle's wheelsets, bogies and car body have three dimensional trajectory movement. Therefore, vertical and lateral accelerations of wheelsets, bogies and car body can be measured at any position. If wheelset, bogies and car body are considered as rigid bodies coupled with springs and dampers, the forces between the track and the vehicle can be determined from the accelerations on rigid bodies [1]. These dynamic forces accelerate the deterioration of track geometry and the presence of rolling contact fatigue type rail defects , e.g. track twists, squats, rail cracks, etc. [2].

The forces required for irregular movements of certain rigid bodies (wheelsets, bogies, car body) are directly proportional to body mass and acceleration according to Newton's laws. Although the mass of the car body is large, its accelerations are usually small. The wheelsets and bogies suffer significant acceleration, the forces required for their displacement ultimately dominate the dynamic forces between the railway vehicle and the track. [3] In this article the relationship between the acceleration of the wheelset and the track irregularities recorded by track geometry measurement is analysed. Vertical irregularities are often caused by an inhomogeneous longitudinal subgrade stiffness/damping distribution. [4]

This paper attempts to determine the relationship between the simultaneously recorded conventional track geometry parameters (longitudinal level, alignment, cross level) and vertical/lateral accelerations of the railway wheelset on straight track segments, i.e., how they are related to forces exerted by irregular vehicle movements that cause further geometric deterioration of the track (Figure 1).

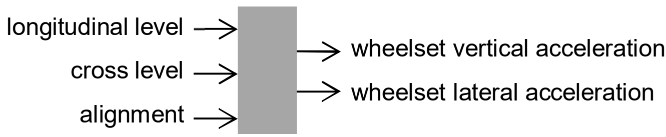

Figure 1. System view of track geometry parameters and wheelset dynamic responses

Nowadays, more and more in-service passenger trains are equipped with inertial sensors providing an useful estimation of the current track quality on daily basis. Therefore, it is important to understand the relationship between ‘vehicle response’ and track geometry deviation from the nominal alignment. [5] [6] [7]. In the past period, track geometry assessment systems of infrastructure managers adopted different theoretical and empirical approaches, and a demand emerged to create an intervention limit system based on dynamical vehicle responses. [8] It is also important to understand the multiplicity of vehicle responses by testing and simulation for the acceptance of running characteristics of railway vehicles. [9]

Based on track geometric irregularities, complex multi-body software is used to estimate acceleration on the vehicle, and the literature deals with the development of so-called performance-based track geometry [10]. The vehicle-track system contains many nonlinearities, and neural networks are particularly suitable for analyzing them. [11]. The recent Dynotrain project also paid particular attention to vehicle reactions to track geometric defects. [12]

2. Methodology

The measurement data required for the experiments now presented were recorded by track geometry measuring system and the vehicle dynamic measurement system operating simultaneously on the measuring car FMK-007, which is originally an intercity wagon and it was adapted for track diagnostic purposes by MÁV Central Rail and Track Inspection Ltd.

The longitudinal level and alignment results used in the experiments now presented are derived from a chord offset measurement system. Therefore, from these measurement results for the correct calculation, the distortion of the chord system has to be compensated by so-called decolouring method. Although European standards [13] require the use of a band-pass filter for a given wavelength range for the assessment of track maintenance measurements, in reality the dynamic response of the vehicle depends on all wavelength components in the track, in this way tests are also performed on decoloured but unfiltered data as well.

2.1. Track geometry measurement data

Track geometry measuring system of the FMK-007 consists of 3 laser units per rail, complemented by an inertial unit between the central laser units. Measurement of longitudinal level and alignment bases on all laser units, as detailed below. Cross level is calculated according to inclination measurement of inertial unit mounted on car body and neighbouring laser sensors compensate for the motion of the car body relative to the rails.

The measuring system works with $\Delta x = 0.25$ m step equidistant sampling. To avoid numerical errors, the lengths of the chord parts for the longitudinal level and alignment resulting from the positioning of the laser units were rounded to 0.25 m. The complex transfer function of the chord system $H(\lambda)$ can be calculated with Eq. (1) known from the literature [14]:

$$H(\lambda) = 1 - \frac{a}{L} e^{\frac{2\pi b}{\lambda} i} - \frac{b}{L} e^{-\frac{2\pi a}{\lambda} i}, \tag{1}$$

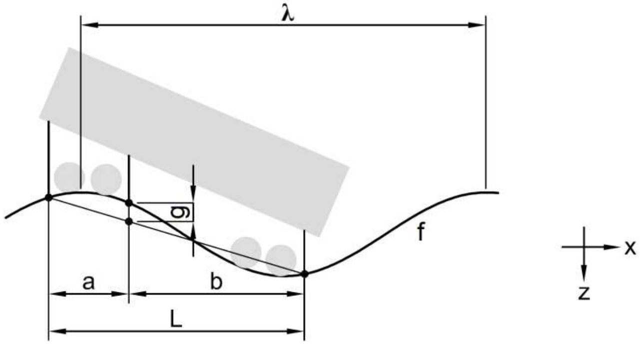

Figure 2. Asymmetric chord offset measurement system of track recording car FMK-007 (drawn by the author)

where the value of *a, b* and *L* (Figure 2) depending on the asymmetric chord are 4.00 m, 19.00 m, 23.00 m, respectively. The parameter λ is the wavelength and *i* is the imaginary unit. In the opposite direction of measurement, *a* and *b* are reversed. The amplitude characteristics (2) and phase characteristics of the system (3) is the same as the magnitude (Figure 3) and phase (Figure 4) of complex function *H*, respectively:

$$|H(\lambda)| = \sqrt{\left[1 - \frac{a}{L}\cos\left(\frac{2\pi}{\lambda}b\right) - \frac{b}{L}\cos\left(\frac{2\pi}{\lambda}a\right)\right]^2 + \left[\frac{b}{L}\sin\left(\frac{2\pi}{\lambda}a\right) - \frac{a}{L}\sin\left(\frac{2\pi}{\lambda}b\right)\right]^2}, \tag{2}$$

$$\angle H(\lambda) = \arctan\frac{\frac{b}{L}\sin\left(\frac{2\pi}{\lambda}a\right) - \frac{a}{L}\sin\left(\frac{2\pi}{\lambda}b\right)}{1 - \frac{a}{L}\cos\left(\frac{2\pi}{\lambda}b\right) - \frac{b}{L}\cos\left(\frac{2\pi}{\lambda}a\right)}, \tag{3}$$

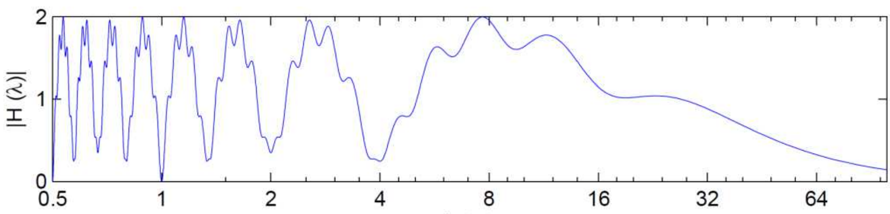

Figure 3. Magnitude of transfer function of the asymmetric chord measurement system (4+19 m)

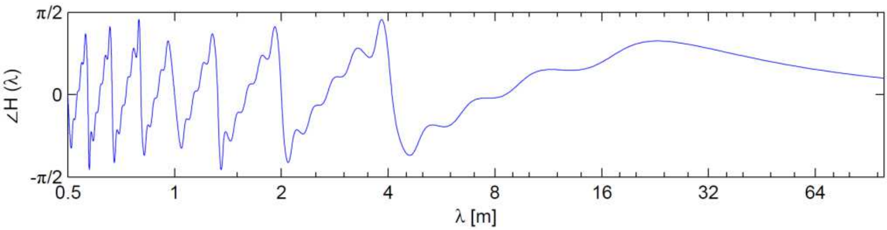

Figure 4. Phase of the transfer function of the asymmetric chord measurement system (4+19m)

The calculations were carried out with data series of straight track section of 1 km, which contained a total of N = 4001 values per measurement parameter. Raw track geometry measurement parameters used:

- cross level (CL),
- longitudinal level of left rail ($LL_{l,chord}$), longitudinal level of right rail ($LL_{r,chord}$),
- alignment of left rail ($AL_{l,chord}$), alignment of right rail ($AL_{r,chord}$).

The data of cross level parameter could be used directly, but for the longitudinal level and alignment parameters had to be decoloured in order to remove the distortion of the chord offset measurement. To do this, the Fourier transform of the sequence must be multiplied by the inverse of the transfer function:

$$F(\lambda) = G(\lambda)\, H^{-1}(\lambda)\,, \tag{4}$$

where F is the Fourier transform of the real track shape labelled with f, and G is the Fourier transform of the measured track geometry data g (which may be $LL_{l,chord}$, $LL_{r,chord}$, $AL_{l,chord}$, $AL_{r,chord}$):

$$G_k = \sum_{n=0}^{N-1} g_n\, e^{-2\pi k \frac{n}{N} i}\,, \tag{5}$$

where $k = 0,1,\ldots N\!-\!1$ and

$$\lambda = \frac{N\,\Delta x}{k}\,, \tag{6}$$

where λ represents considered wavelength. (If $k = 0$, then the general shift of g is in question.)

Reciprocating by definition

$$H^{-1} = \frac{\mathrm{Re}(H) - i\,\mathrm{Im}(H)}{|H|^2}, \tag{7}$$

at low values of $|H|$ makes the calculation numerically unstable and it cannot be applicable if zero value is used. Managing this problem requires great care, as *H* needs to be modified and this also affects the result. According to *Insa* [15] complex numbers less than a given value should be replaced by 1. However, in this study, in case of $|H| < c$ the Eq. (7) was modified as follows:

$$H^{-1}_{|H|<c} = \frac{\mathrm{Re}(H) - i\,\mathrm{Im}(H)}{c^2}, \tag{8}$$

where *c* is 0.2, determined after multiple trials. The decoloured parameter *f* (which may be LL_r, LL_l, AL_r, AL_l), was calculated using (4) and after that an inverse-Fourier transform was performed on function *F(λ)*:

$$f_n = \frac{1}{N} \sum_{k=0}^{N-1} F_k \; e^{2\pi k \frac{n}{N} i}\,, \tag{9}$$

Of the converted 1 km track section, only the middle 800 m could be used well because of numerical issues.

On function *f*, the band-pass filtering for D1 wavelength range (3 m < λ < 25 m) according to EN 13848 [13] resulted in sequences $LL_{r,D1}$, $LL_{l,D1}$, $AL_{r,D1}$, $AL_{l,D1}$.

2.2. Acceleration measurement data

In this paper only some accelerometer sensors of the vehicle dynamic measurement system of the car FMK-007 were used. The accelerometer sensors located at the axlebox of leading wheelset considering the measurement direction was taken into account. Positioning of sensors are (Figure 5):

- there are one-axle vertical accelerometer sensors above the axleboxes on both sides of the leading wheelset, the labelling of which are $\ddot{z}_l$ and $\ddot{z}_r$,
- there is a one-axle lateral accelerometer sensor above the axlebox on left side of the wheelset, the labelling of which is $\ddot{y}$.

The accelerometer sensors are located at a height of *h* = 0.65 m above the rail top level on a vertical console attached to the end of the axlebox (Figure 6), the distance between the vertical accelerometers is *q* = 2.5 m, the average distance of the wheel-rail contact patches is *t* = 1.5 m. During the study, it was focused on the relevant wavelengths of track geometry, which starts, according to Salvador [16] at around 2 metres. There was no goal to investigate rail surface defects (e.g. squat). Therefore, the acceleration signals were passed through a 16 Hz second-order Butterworth low-pass filter and recorded at 300 Hz sampling rate (gain: ± 100g).

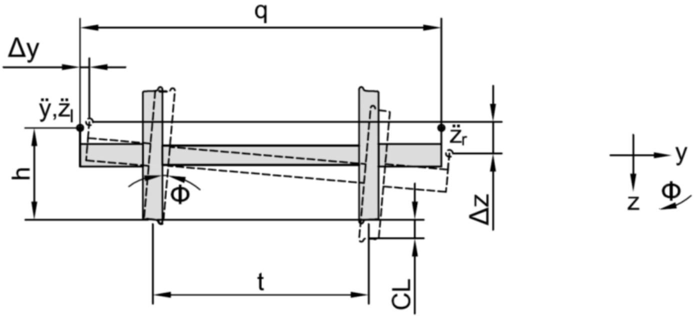

Figure 5. Accelerometer sensors $\ddot{y}$, $\ddot{z}_l$, $\ddot{z}_r$ mounted above the axleboxes and visualization of rotated wheelset due to cross level defect (drawn by the author)

Figure 6. Accelerometer sensor box mounted above the axlebox (photo taken by the author)

2.3. Connection between lateral and vertical axlebox accelerations

In the case of level irregularity of one of the rails, due to the change in the cross level *CL* the wheelset is rotated around one rail as marked by *Φ* in Figure 5. Because of small angles:

$$CL \approx \mathrm{t}\,\phi\,, \tag{10}$$

height difference between vertical accelerometers located above the end of the axleboxes:

$$\Delta z \approx \mathrm{q}\,\phi\,, \tag{11}$$

lateral displacement of the accelerometer mounted on the axlebox at height h:

$$\Delta y \approx \mathrm{h}\, \phi\,. \tag{12}$$

Therefore, the following relationship can be assumed between the vertical axlebox acceleration and the lateral axlebox acceleration when passing through a track twist:

$$\ddot{y}_{\Delta\ddot{z}} = \frac{\mathrm{h}}{\mathrm{q}}(\ddot{z}_l - \ddot{z}_r)\,. \tag{13}$$

2.4. Axlebox acceleration calculation based on track geometry data

If the wheels 'follow' the rail irregularities perfectly, the trajectory movement of the wheels will be same as the track geometry which is recorded. If a constant measuring speed is assumed, the accelerations of the wheelset can be calculated based on track geometry results by double deriving. [17] Taking into account the actual speed, an estimation was made for the axlebox acceleration. Compared to the acceleration signals, it was found that the $\Delta x = 0.75$ m step is the most favourable for numerical derivation. Derivatives are:

$$f'(x) = \frac{f(x+\Delta x) - f(x)}{\Delta x}, \tag{14}$$

$$f''(x) = \frac{f(x+\Delta x) - 2f(x) + f(x-\Delta x)}{\Delta x^2}, \tag{15}$$

$$f'''(x) = \frac{f(x+2\Delta x) - 3f(x+\Delta x) + 3f(x) - f(x-\Delta x)}{\Delta x^3}, \tag{16}$$

where $f^{(n)}(x)$ is the *n*-order derivative of a track geometry parameter at section x and $f(x - \Delta x)$, $f(x + \Delta x)$ are the values of *LL, AL, CL,* 0.75 m before and after section x, respectively.

The resulting acceleration is proportional to the square of the speed. The expected track acceleration based on track geometry is therefore calculated by following equations. Considering the permanent travel speed v, the estimate of left vertical wheel acceleration based on the left longitudinal level is:

$$\ddot{z}_{l,LL,l} = LL_l''(x)\, v^2. \tag{17}$$

Taking into account the permanent travel speed, the estimate of lateral wheelset acceleration based on the left alignment is (assuming that wheelset directly 'follows' lateral track irregularities):

$$\ddot{y}_{AL,l} = AL_l''(x)\, v^2, \tag{18}$$

Taking into account the permanent travel speed, accelerometer positioning and wheelset measures, the estimate of lateral wheelset acceleration based on cross level is:

$$\ddot{y}_{CL} = \frac{\mathrm{h}}{\mathrm{t}} CL''(x)\, v^2. \tag{19}$$

Because of noise, the value of $\ddot{y}_{cl}$ was smoothed by a 0.75 m moving average.

2.5. Calculation of correlation coefficient

When acceleration signals were compared to track geometry measurements, a resampling of 0.25 m step was performed on the acceleration data. Synchronisation of signals was carried out manually. The method of calculating the correlation coefficient was the same as that used by *Karis et al.* [18]:

$$r_{u,v} = \frac{\mathrm{cov}(u,v)}{\sigma_u \sigma_v} = \frac{\sum_{j=1}^{N}(u_j-\bar{u})(v_j-\bar{v})}{\sqrt{\sum_{j=1}^{N}(u_j-\bar{u})^2 \sum_{j=1}^{N}(v_j-\bar{v})^2}}. \tag{20}$$

3. Results

3.1. Correlation between vertical and lateral axlebox accelerations

Correlations between vertical and lateral axlebox accelerations were investigated on a Hungarian railway line (Budapest–Kelebia), with variable measurement speeds (0–80 km/h), omitting the curved sections, over 45 km length, as well as over 1 km long straight section with constant speed of 79 km/h (Table 1).

The standard deviation of the decoloured and D1 filtered parameters on the examined 1 km long section is given as follows. Standard deviations (in millimetres) of left longitudinal level, right longitudinal level, left alignment, right alignment are 2.71, 2.33, 1.22 and 1.28, respectively.

The correlation coefficient between $\ddot{z}_l - \ddot{z}_r$ and $\ddot{y}$, over the tested 45 km inhomogeneous and variable speed section is 0.75 and over the 1 km homogeneous section 0.79. There is also connection between $\ddot{y}$ and separately recorded vertical axlebox accelerations. The lateral accelerometer is located on the left side and the numbers indicate that the connection with the left vertical accelerometer shows higher correlation.

Table 1. Correlation coefficients between vertical and lateral wheelset accelerations (45 km various track and various measuring speeds)

	45 km track, various speed	*1 km track, constant speed*
	$\ddot{\boldsymbol{y}}$ [m/s^2]	
$\ddot{z}_r$ [m/s^2]	–0.39	–0.57
$\ddot{z}_l$ [m/s^2]	0.46	0.68
$\ddot{z}_l - \ddot{z}_r$ [m/s^2]	**0.75**	**0.79**

Figure 7 shows the measured and the estimated lateral axlebox acceleration which was calculated by Eq. (13) based on $\ddot{z}_l - \ddot{z}_r$.

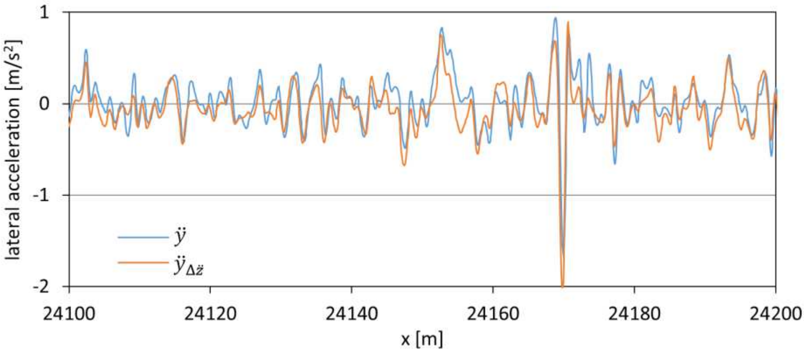

Figure 7. Measured lateral axlebox acceleration and estimated wheelset lateral acceleration based on vertical axlebox acceleration difference

3.2. Correlation between vertical axlebox accelerations and longitudinal level

Correlation coefficients were calculated for the 1 km (800 m) long section detailed above, comparing the left axlebox acceleration and the left longitudinal level (Table 2).

The acceleration measured on the left axlebox correlates with the second order derivative of the de-coloured left longitudinal level (LL_l'') significantly (0.63). The correlation with the second order derivative of the original chord measurement data is close to this (0.56). The statistical relationship to the D1 filtered data is in low level.

Table 2. Correlation coefficients between vertical axlebox accelerations and longitudinal level derivatives (0.8 km track, 79 km/h speed)

	$\ddot{z}_l$ [m/s²]
$LL_{l,chord}$ [mm]	0.40
$LL''_{l,chord}$ [mm]	0.56
$LL_{l,D1}$ [mm]	0.21
$LL''_{l,D1}$ [mm]	0.14
LL_l [mm]	0.38
LL'_l [mm]	0.42
LL''_l [mm]	**0.63**
LL'''_l [mm]	0.43

A Figure 8 shows the measured left vertical axlebox acceleration and the estimated left lateral wheel acceleration which was calculated by Eq. (17) based on LL''_l. It should be taken into consideration that the vertical acceleration and the longitudinal level were measured in two separate planes: at the axleboxes and at the rail, respectively.

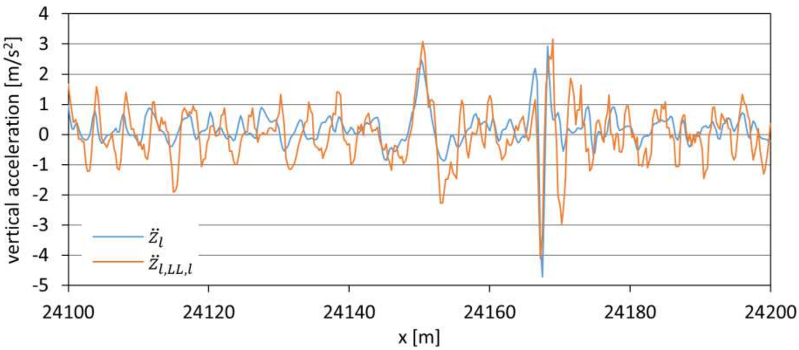

Figure 8. Measured vertical axlebox acceleration and estimated vertical wheel acceleration based on longitundinal level (left)

3.3. Correlation between lateral axlebox acceleration and alignment and cross level

Correlation coefficients were calculated for the 1 km (800 m) long section detailed above, for the cross level and for left alignment (Table 3). In the alignment parameter, neither the original chord nor the decoloured data showed a noticeable statistical relationship with the lateral axlebox acceleration, not even the second derivative. However, the second order derivative of the cross level is closely related to the lateral axlebox acceleration, where the correlation coefficient is 0.77. First order derivative of cross level (CL') was also calculated, which corresponds to traditional 'track twist' on 0.75 m base, but its correlation is weaker.

Table 3. Correlation between vertical axlebox acceleration and alignment and cross level (0.8 km track, 79 km/h speed)

	$\ddot{\boldsymbol{y}}$ [m/s^2]
$AL_{l,chord}$ [mm]	0.07
$AL_{r,chord}$ [mm]	0.12
$AL''_{l,chord}$ [mm]	–0.02
$AL''_{r,chord}$ [mm]	0.05
$AL_{l,D1}$ [mm]	0.02
$AL_{r,D1}$ [mm]	0.05
$AL''_{l,D1}$ [mm]	–0.07
$AL''_{r,D1}$ [mm]	0.02
AL_l [mm]	0.07
AL_r [mm]	0.09
AL''_l [mm]	0.02
AL''_r [mm]	0.03
CL [mm]	0.35
CL' [mm]	0.53
CL'' [mm]	**0.77**
CL''' [mm]	0.60

Figure 9 shows the measured lateral axlebox acceleration and the estimated lateral axlebox acceleration which was calculated by Eq. (18) based on AL''_l and the estimated lateral axlebox acceleration which was calculated by Eq. (19) based on CL''.

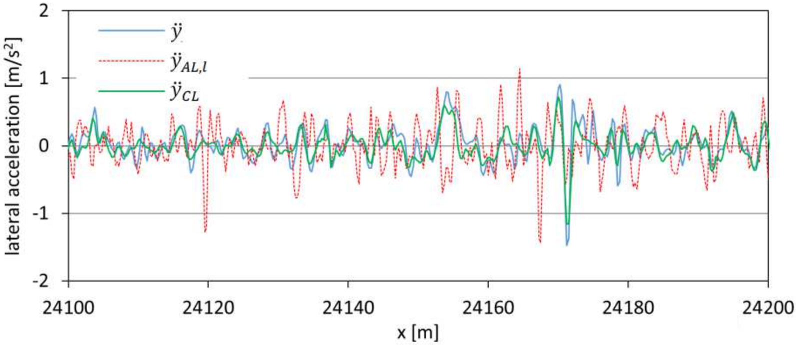

Figure 9. Measured lateral axlebox acceleration and estimated lateral acceleration based on alignment (left) and cross level

4. Conclusions

For economical track maintenance it is important to understand the relationship between the irregularities recorded by conventional track geometry measuring car and the resulting dynamic vehicle responses. The conclusions reached in this article are based on experiment carried out on only straight track in average condition which contains only stochastic track geometry irregularities but no curves or transition curves.

The difference of the signals of the vertical accelerometers (mounted above the left and right axleboxes) correlated with the signal of the lateral axlebox accelerometer significantly. Therefore, it can be concluded that the lateral accelerations of the axlebox are decisively influenced by the roll movements of the wheelset resulting from rate of the change of cross level. The differences of the vertical axlebox accelerations and the lateral axlebox acceleration are practicably proportional, and the proportionality constant results come from the geometric position of the accelerometers.

Based on the correlation analysis of the longitudinal level and the measured vertical accelerations it can be stated that the highest correlation was found in case the chord measurement was decoloured using the inverse of the transfer function and the second derivative of the resulting data series was produced. This means that the amplitude-based local fault evaluation used in the current track maintenance practice is not entirely adequate to limit the force exerted in the vehicle-track system, but rather the second order derivative of the longitudinal level. This coincides with the often stated statement in the international and Hungarian literature: not only the amplitude of the local defect, but also its 'wavelength' is essential. However, based on the present study, it can be said that second order derivative is determinant. The optimum step of numerical derivation from the point of view of correlation is believed to depend on the speed of the vehicle and the low pass filtering rate applied on the acceleration signals: for 80 km/h and 16 Hz low-pass filter frequency a step of 0.75 m was favourable. Vertical acceleration and the longitudinal level were measured in two separate planes, in this way left axlebox acceleration could be influenced by both left and right longitudinal level.

Filtering to the D1 wavelength range greatly reduces the correlation between longitudinal level and measured vertical accelerations. This is explained by the fact that larger accelerations occur in short-wave track geometry defects that are reduced or eliminated by D1 filtering.

On the straight line examined, the lateral axlebox acceleration and any derivatives of the alignment parameters appeared to be statistically independent. This is due to the fact that the wheelset does not directly 'follow' the stochastic lateral rail irregularities with small amplitude, so there is no linear statistical relationship between the two sets of data. Small alignment irregularities cause only wheel-rail contact patch displacement, not a lateral wheelset displacement.

On the basis of the calculated correlation between the cross level derivatives and the lateral axlebox acceleration, it can be concluded that the lateral accelerations of wheelsets (and bogies) were influenced by the cross level changes primarily. The first derivative of the cross level (which is similar to the 'track twist') produced a lower level correlation, but based on the second derivative of the cross level, the lateral axlebox acceleration can be estimated well. Therefore, it is also advisable to consider the second order derivatives of the cross level for the analysis of the effects from vehicle on the track. Cross level defects can therefore cause not only vertical extra forces but significant lateral forces as well. From the point of view of safety against derailment, the lateral force component between the wheel and the rail is of key importance and attention should be paid.

However, the author dealt only straight tracks in this article, in the future dynamic parameters are able to be analysed not only on straight track, but also in curves and transition curves. The European railway track design standard [19] contains the calculation possibility (method) of different dynamic parameters (eg. 'angular acceleration around roll axis', 'angular jerk around roll axis'). Some researchers investigated the transition curves from geometrical and design aspects [20] which results can be used in the future analyses.

References

[1] L. Császár, Cs. Pálfi: Determination of the wheel/rail contact forces by different measurement methods, in: Proceedings of the 9th International Conference on Railway Bogies and Running Gears, Budapest, Hungary, 2013, pp. 153–166.

[2] M. Molodova, Z. Li, R. Dollevoet: Axlebox acceleration: Measurement and simulation for detection of short track defects. Wear 271 (1-2) (2011) pp. 349–356.
doi: http://dx.doi.org/10.1016/j.wear.2010.10.003

[3] A. Haigermoser, B. Luber, J. Rauh, G. Gräfe: Road and track irregularities: measurement, assessment and simulation. Vehicle System Dynamics 53 (7) (2015) pp. 878–957.
doi: http://dx.doi.org/10.1080/00423114.2015.1037312

[4] V. Zoller, I. Zobory: On dynamics of the track/vehicle system in presence of inhomogeneous rail supporting parameters. Periodica Polytechnica Transportation Engineering 39 (2) (2011) pp. 83–85.
doi: http://dx.doi.org/10.3311/pp.tr.2011-2.06

[5] P. Weston, C. Roberts, G. Yeo, E. Stewart: Perspectives on railway track geometry condition monitoring from in-service railway vehicles. Vehicle System Dynamics, 53 (7) (2015) pp. 1063–1091.
doi: http://dx.doi.org/10.1080/00423114.2015.1034730

[6] X. Wei, F. Liu, L. Jia: Urban rail track condition monitoring based on in-service vehicle acceleration measurements. Measurement 80 (2016) pp. 217–228.
doi: http://dx.doi.org/10.1016/j.measurement.2015.11.033

[7] Á. Vinkó, P. Bocz, Z. Posgay: A practical approach to tramway track condition monitoring: vertical track defects detection and identification using timefrequency processing techniques. SSP – Journal of Civil Engineering, 13 (s1) (2018) pp. 135–146.
doi: http://dx.doi.org/10.1515/sspjce-2018-0013

[8] Sz. Fischer, F. Horvát: Speed-dependence of railway superstructure's geometric tolerances, in: G. Köllő (Ed.) XIII. Nemzetközi Építéstudományi Konferencia: ÉPKO 2009, Cluj-Napoca, Romania, 2009, pp. 137–143, in Hungarian.

[9] European Standard EN 14363. Testing and Simulation for the acceptance of running characteristics of railway vehicles. Running Behaviour and stationary tests.

[10] Y. Liu, E. Magel: Performance-based track geometry and the track geometry interaction map. Proceedings of the Institution of Mechanical Engineers, Part F: Journal of Rail and Rapid Transit 223 (2) (2009) pp. 111–119. doi: http://dx.doi.org/10.1243/09544097JRRT225

[11] T. Karis: Correlation between Track Irregularities and Vehicle Dynamic Response Based on Measurements and Simulations. Doctoral dissertation, KTH Royal Institute of Technology (2018).

[12] K. U. Wolter, M. Zacher, B. Slovak: Correlation between track geometry quality and vehicle reactions in the virtual rolling stock homologation process, in: 9th World Congress on Railway Research, 2011, pp. 22–26.

[13] European Standard EN 13848. Railway applications. Track. Track geometry quality.

[14] B. Lichtberger: Track compendium. EurailPress, Hamburg, 2005, pp. 400–405.

[15] R. Insa, J. Inarejos, P. Salvador, L. Baeza: On the filtering effects of the chord offset method for monitoring track geometry. Proceedings of the Institution of Mechanical Engineers, Part F: Journal of Rail and Rapid Transit 226 (6) (2012) pp. 650–654. doi: http://dx.doi.org/10.1177/0954409712447481

[16] P. Salvador, V. Naranjo, R. Insa, P. Teixeira:. Axlebox accelerations: Their acquisition and time–frequency characterisation for railway track monitoring purposes. Measurement 82 (2016) pp. 301–312. doi: http://dx.doi.org/10.1016/j.measurement.2016.01.012

[17] M. Li, I. Persson, J. Spännar, M. Berg: On the use of second-order derivatives of track irregularity for assessing vertical track geometry quality. Vehicle System Dynamics 50 (sup1) (2012) pp. 389–401.
doi: http://dx.doi.org/10.1080/00423114.2012.671947

[18] T. Karis, M. Berg, S. Stichel, M. Li, D. Thomas, B. Dirks: Correlation of track irregularities and vehicle responses based on measured data. Vehicle System Dynamics 56 (6) (2018) pp. 967–981.
doi: http://dx.doi.org/10.1080/00423114.2017.1403634

[19] European Standard EN 13803:2017. Railway applications. Track. Track alignment design parameters. Track gauges 1435 mm and wider.

[20] Sz. Fischer: Comparison of railway track transition curves. Pollack Periodica 4 (3) (2009) pp. 99–110.
doi: https://doi.org/10.1556/Pollack.4.2009.3.9